DMD Fast Forward. Published on October 29, 2024 as DOI: 10.1124/dmd.124.001895
This article has not been copyedited and formatted. The final version may differ from this version.

Title

Pharmacokinetics and ADME Profiling of Tanimilast Following an Intravenous ^{14}C-Microtracer co-administered with an Inhaled Dose in Healthy Male Individuals

Authors

Michele Bassi[1], Veronica Puviani[1], Debora Santoro[1], Sonia Biondaro[1], Aida Emirova[2], Mirco Govoni[1]

1. Global Clinical Development, Chiesi Farmaceutici SpA, Parma, Italy;

2. Global Clinical Development, Chiesi S.A.S., Bois Colombes, France

Downloaded from dmd.aspetjournals.org at ASPET Journals on December 20, 2024

DMD Fast Forward. Published on October 29, 2024 as DOI: 10.1124/dmd.124.001895
This article has not been copyedited and formatted. The final version may differ from this version.

Running title

Pharmacokinetics and ADME Characterization of Tanimilast

Corresponding author

Michele Bassi

Global Clinical Development, Chiesi Farmaceutici SpA,

Largo Francesco Belloli 11/A - 43122 Parma (Italy)

Tel: +39 0521 1689 570

Email: m.bassi@chiesi.com

Text pages: 22 (abstract to discussion)

Figures: 4

Tables: 2

Supplemental tables: 0

Supplemental figures: 0

References: 37

Word count, Abstract: 247/250

Word count, Introduction: 638/750

Word count, Discussion: 1500/1500

Downloaded from dmd.aspetjournals.org at ASPET Journals on December 20, 2024

DMD Fast Forward. Published on October 29, 2024 as DOI: 10.1124/dmd.124.001895
This article has not been copyedited and formatted. The final version may differ from this version.

Abstract

Tanimilast is an inhaled phosphodiesterase-4 inhibitor currently in phase 3 clinical development for treating chronic obstructive pulmonary disease (COPD) and asthma. This trial aimed to characterize the pharmacokinetics, mass balance, and metabolite profiling of tanimilast. Eight healthy male volunteers received a single dose of non-radiolabeled tanimilast via powder inhaler (NEXThaler® (3200μg)), followed by a concomitant intravenous (IV) infusion of a microtracer ([^{14}C]-tanimilast: 18.5μg and 500nCi). Plasma, whole blood, urine, and feces samples were collected up to 240 hours post-dose to quantify non-radiolabeled tanimilast, [^{14}C]-tanimilast, and total-[^{14}C]. The inhaled absolute bioavailability of tanimilast was found to be approximately 50%. Following IV administration of [^{14}C]-tanimilast, plasma clearance was 22 L/h, the steady-state volume of distribution was 201 L, and the half-life was shorter compared to inhaled administration (14 vs. 39 hours, respectively), suggesting that plasma elimination is limited by the absorption rate from the lungs. 79% (71% in feces; 8% in urine) of the IV dose was recovered in excreta as total-[^{14}C]. [^{14}C]-tanimilast was the major radioactive compound in plasma, while no recovery was observed in urine and only 0.3% was recovered in feces, indicating predominant elimination through metabolic route. Importantly, as far as no metabolites accounting for more than 10% of the circulating drug-related exposure in plasma or the administered dose in excreta were detected, no further qualification is required according to regulatory guidelines. This study design successfully characterized the absorption, distribution, and elimination of tanimilast, providing key pharmacokinetic parameters to support its clinical development and regulatory application.

Downloaded from dmd.aspetjournals.org at ASPET Journals on December 20, 2024

DMD Fast Forward. Published on October 29, 2024 as DOI: 10.1124/dmd.124.001895
This article has not been copyedited and formatted. The final version may differ from this version.

Significance Statement

This trial investigates PK and ADME profile of tanimilast, an inhaled PDE4 inhibitor for COPD and asthma. Eight male volunteers received a dose of non-radiolabeled tanimilast via NEXThaler® and a microtracer IV dose. Results show pivotal PK results for the characterization of tanimilast, excretion route and quantification of significant metabolites, facilitating streamlined clinical development and regulatory approval.

Downloaded from dmd.aspetjournals.org at ASPET Journals on December 20, 2024

DMD Fast Forward. Published on October 29, 2024 as DOI: 10.1124/dmd.124.001895
This article has not been copyedited and formatted. The final version may differ from this version.

Abbreviations

^{14}C Carbon-14

ADME absorption, distribution, metabolism and excretion

AMS accelerator mass spectrometry;

AUC area under the curve;

AUC_{0-t} the area under the concentration-time curve from dosing to the last quantifiable concentration;

BCRP breast cancer resistance protein;

CL total body plasma clearance;

C_{max} the value of maximum plasma concentration;

COPD Chronic Obstructive Pulmonary Disease;

CV% percentage of coefficient of variation;

E_h hepatic extraction ratio;

EMA European Medicines Agency;

F absolute inhaled bioavailability;

FDA U.S. Food and Drug Administration;

ICH International Council for Harmonization;

IV intravenous;

LC liquid chromatography;

LLOQ lower limit of quantification;

MRT mean residence time of the drug in the systemic circulation;

MS mass spectrometry;

PDE4 phosphodiesterase-4;

pg Eq/mL picogram tanimilast equivalents per mL;

P-gp P-glycoprotein;

PK pharmacokinetics;

$t_{1/2}$ terminal phase half-life;

t_{max} time from dosing of the maximum plasma concentration;

Vss volume of distribution at steady state;

Vz volume of distribution;

Downloaded from dmd.aspetjournals.org at ASPET Journals on December 20, 2024

DMD Fast Forward. Published on October 29, 2024 as DOI: 10.1124/dmd.124.001895
This article has not been copyedited and formatted. The final version may differ from this version.

Introduction

Tanimilast (international non-proprietary name (INN) of CHF6001 or (S)-3,5-dichloro-4-(2-(3-(cyclopropylmethoxy)-4-(difluoromethoxy)phenyl)-2-(3-(cyclopropylmethoxy)-4-(methylsulfonamido)benzoyloxy)ethyl)pyridine1-oxide) is an inhaled phosphodiesterase-4 inhibitor, a non-steroidal anti-inflammatory drug currently advancing through Phase III clinical trials. This novel compound aims to reduce exacerbation risk in Chronic Obstructive Pulmonary Disease (COPD) patients with chronic bronchitis phenotype and a history of exacerbations when added to triple therapy (ClinicalTrials.gov NCT04636801 [PILASTER] and NCT04636814 [PILLAR]). Additionally, its potential in treating asthma is currently being evaluated in Phase II study (NCT06029595 [TANGO]). Results from the early tanimilast development studies have demonstrated promising pharmacodynamic and efficacy outcomes, coupled with a favorable safety profile, highlighting the absence of class-related side effects associated with phosphodiesterase-4 inhibitors (Singh *et al.*, 2016, 2019, 2021; Govoni *et al.*, 2020, 2023; Singh, Emirova, *et al.*, 2020; Singh, Watz, *et al.*, 2020).

The pharmacokinetic (PK) profile of tanimilast has been examined through various studies at repeated doses up to 4800 µg/day (Facchinetti *et al.*, 2021). These include single and multiple ascending dose studies in healthy subjects (Mariotti *et al.*, 2018) and two double-blind, placebo-controlled, 3-way crossover studies in mild allergic asthma and COPD patients involving repeated doses (Singh *et al.*, 2016, 2019) . These investigations have revealed a clear correlation between doses and plasma concentrations, further supported by pharmacokinetic modeling analyses indicating no time dependency in PK parameters (Jolling *et al.*, 2019).

These studies offer valuable insights into the pharmacokinetics of tanimilast. However, a crucial aspect in both drug development (Penner *et al.*, 2009; Young *et al.*, 2023) and the regulatory approval process (Coppola *et al.*, 2019) is the comprehensive investigation of absorption, distribution, metabolism and excretion (ADME) through a radiolabeled mass balance clinical study. It is particularly imperative to characterize metabolites, especially

Downloaded from dmd.aspetjournals.org at ASPET Journals on December 20, 2024

DMD Fast Forward. Published on October 29, 2024 as DOI: 10.1124/dmd.124.001895
This article has not been copyedited and formatted. The final version may differ from this version.

those constituting more than 10% of circulating drug-related exposure in plasma or of the administered dose in excreta, requiring additional characterization and toxicology studies (https://www.fda.gov/regulatory-information/search-fda-guidance-documents/safety-testing-drug-metabolites).

This study adopts an innovative clinical approach by administering an intravenous (IV) [^{14}C]-labeled microtracer concomitantly with the pharmacological dose via inhalation (Lappin, 2016). The microtracer approach, involving subpharmacologic administration (1% of the pharmacologic dose or 100 µg, whichever is lower) (https://www.fda.gov/regulatory-information/search-fda-guidance-documents/microdose-radiopharmaceutical-diagnostic-drugs-nonclinical-study-recommendations, https://database.ich.org/sites/default/files/M3_R2__Guideline.pdf) and less than 1000 nCi of radioactive dose (https://www.fda.gov/regulatory-information/search-fda-guidance-documents/clinical-pharmacology-considerations-human-radiolabeled-mass-balance-studies), presents advantages over traditional crossover Phase I studies (Spracklin *et al.*, 2020; Young *et al.*, 2024), avoiding the need for intravenous toxicology programs and dosimetry studies in animals. Considering the very low amount of radioactivity administered, the highly sensitive Accelerator Mass Spectrometry (AMS) quantifies the [^{14}C]-microtracer, while the non-radiolabeled dose's PK is assessed through traditional liquid chromatography tandem mass spectrometry (LC-MS/MS) assay (Young and Croft, 2020).

For ADME characterization, intravenous dosing serves as a surrogate for the drug's systemic circulation after absorption from the lung (Ambery *et al.*, 2018; Harrell *et al.*, 2019; Holmberg *et al.*, 2022). This strategic choice arises due to complications associated with inhaled [^{14}C]-labeled compounds, such as formulation feasibility and accurate dose quantification, crucial for measuring total dose recovery in excreta. Additionally, long-term toxicological effects of [^{14}C] in the lung are not known.

Preceding studies involving intravenous administration of radiolabeled [^{14}C]-tanimilast in rats disclosed widespread distribution, with peak concentrations in the liver, kidney, pancreas, and spleen after 1 hour, and in the lung after 4 hours. Excretion was rapid, as more than

Downloaded from dmd.aspetjournals.org at ASPET Journals on December 20, 2024

DMD Fast Forward. Published on October 29, 2024 as DOI: 10.1124/dmd.124.001895
This article has not been copyedited and formatted. The final version may differ from this version.

79% of the dose was eliminated within 48 hours, with no increasing within 120h. The main elimination route of radioactivity was via feces (around 80%) whereas less than 5% was found in urine. Biliary excretion's pivotal role was also confirmed, recovering over 90% of the administered radioactive dose (Cenacchi et al., 2018 and unpublished Chiesi data).

This paper details a pivotal clinical Mass Balance study (ClinicalTrials.gov NCT04756960) conducted in healthy subjects, aiming to provide essential information on tanimilast's exposure, both as the parent compound and its metabolites. The study's objectives encompass evaluating the pharmacokinetics of tanimilast, characterizing the mass balance, and elucidating the relevant metabolites in humans.

Downloaded from dmd.aspetjournals.org at ASPET Journals on December 20, 2024

DMD Fast Forward. Published on October 29, 2024 as DOI: 10.1124/dmd.124.001895
This article has not been copyedited and formatted. The final version may differ from this version.

Materials and Methods

Tanimilast for inhalation, as well as reference standards for tanimilast and its known metabolites (CHF5956 and CHF5928), were provided by Chiesi Farmaceutici (Parma, Italy). [^{14}C]-tanimilast, with a specific radioactivity of 27 nCi/µg (0.10 kBq/µg), was supplied by Quotient Sciences (Alnwick, UK), by a chemical synthesis previously described (Fontana *et al.*, 2017). This material was manufactured under Good Manufacturing Practice and formulated into a solution at a concentration of 1.79 µg/mL (49.66 nCi/mL) in ethanol (2% v/v) and Kolliphor HS 15 (2% v/v), dissolved in a 0.9% w/v sodium chloride solution for IV infusion by the Fortrea Clinical Research Unit (Leeds, UK). All other solvents and reagents utilized in this study were of analytical grade and procured from commercial suppliers.

Study Design

This clinical trial constituted a Phase I study conducted at a single center, Fortrea Clinical Research Unit (CRU), Leeds (UK), from March 2021 to April 2021. The design involved a single dose, non-randomized, open-label, uncontrolled approach. The trial adhered to the Declaration of Helsinki and its latest revision, as well as the International Council for Harmonisation (ICH) E6 Good Clinical Practice (GCP) guideline. Approval was obtained from the North East–York Research Ethics Committee and by the Administration of Radioactive Substances Advisory Committee, and all subjects provided written informed consent before participating in any study-related procedures.

Following the screening visit, eligible subjects entered the study, which consisted of a single-dose treatment period. On Day 1 of the treatment period, participants received four inhalations of tanimilast via the NEXThaler® multi-dose dry-powder inhaler (total inhaled dose: 3200 µg). This inhalation was followed by a 15-minute intravenous infusion of the microtracer, involving the injection of 10 mL of [^{14}C]-tanimilast, concluding at the expected time to maximum concentration (t_{max}) of 2 hours for the inhaled dose. This timing aimed to minimize any potential non-linear pharmacokinetic effects. The total infused dose was 18.5 µg and 500 nCi (18.5 kBq). Inhaled drug administration occurred under fasting conditions (at

Downloaded from dmd.aspetjournals.org at ASPET Journals on December 20, 2024

DMD Fast Forward. Published on October 29, 2024 as DOI: 10.1124/dmd.124.001895
This article has not been copyedited and formatted. The final version may differ from this version.

least 10 hours fasting prior to administration), and subjects remained fasted until 2 hours post-dose. Subjects were continuously supervised by medical staff at the clinical site until the morning of Day 11, upon which they were discharged following the completion of 240 hours post-dose (IV) assessments on Day 11. The 240-hour post-dose collection interval was selected to exceed five times the half-life of inhaled tanimilast as measured in previous clinical trials (Mariotti *et al.*, 2018). A follow-up phone call was conducted 7 to 10 days after discharge to document concomitant medications and assess the status of any unresolved or new adverse events.

Throughout the study, each subject received an effective radioactive dose of 0.005 millisieverts, well within the safety limits defined by the World Health Organization category 1 and the International Commission on Radiologic Protection category 1 (<0.1 millisievert; minor risk) (International Commission on Radiological Protection, 1991). The administered radioactivity was categorized as a microtracer dose, containing 18.5 kBq (500 nCi) of [^{14}C].

Study Population

The study enrolled physically healthy male individuals aged between 30 and 55 years inclusive, exhibiting a body mass index within the range of 18 to 35 kg/m^2 inclusive, and with regular bowel movements. Inclusion criteria required participants to have no history of substance abuse, including drug or alcohol, no smoking habits and no clinically significant medical conditions. Intake of any enzyme-inducing drugs, enzyme-inhibiting drugs, biologic drugs or any drug known to have a well-defined potential for hepatotoxicity were not permitted within 3 months prior to screening and throughout the study period. Additionally, eligible individuals had not been exposed to significant radiation diagnostic or therapeutic radiation (eg, serial X-ray, computed tomography scan, barium meal) in the 12 months preceding the study. Participants were confined to the study center for the entire duration of the research. Comprehensive details regarding the eligibility criteria are available on ClinicalTrials.gov under the identifier NCT04756960.

Downloaded from dmd.aspetjournals.org at ASPET Journals on December 20, 2024

DMD Fast Forward. Published on October 29, 2024 as DOI: 10.1124/dmd.124.001895
This article has not been copyedited and formatted. The final version may differ from this version.

Sample Collection

For tanimilast analysis in plasma, samples were collected before dosing (within 60 min from inhaled dosing) and at 15, 30, 60, 90 min, 2, 3.75, 5.75, 7.75, 9.75, 11.75, 13.75, 25.75, 49.75, 73.75, 97.75, 121.75, 145.75, 169.75, 193.75, 217.75 and 241.75 hours postdose. For [^{14}C]-tanimilast, total-[^{14}C] analysis and quantitative profiling of metabolites in plasma, samples were collected before dosing (within 60 min from inhaled dosing) and at the following timepoints relative to the start of the IV infusion: 5, 10, 15 [end of infusion], 20, 25, 30, 45, 60 min, 2, 4, 6, 8, 10, 12, 24, 48, 72, 96, 120, 144, 168, 192, 216 and 240 hours. Urine samples were obtained at predose and at specific time intervals relative to the initiation of the IV infusion: 0-4h, 4-8h, 8-12h, 12-24h post-dose on the first day, and subsequently in 24-hour intervals up to 240 hours. Fecal samples were collected both pre-dose and at 24-hour intervals up to 240 hours.

Mass Balance

Fecal and urine samples were transported and analyzed at Pharmaron ABS (Germantown, Maryland, USA). For each pooled feces sample, homogenization was achieved by adding deionized water at a ratio ranging from approximately 1:1 to 1:2 (w/w), adjusted based on the bulk sample's consistency. All contemporary biological samples contain background [^{14}C]. The amount of background [^{14}C] present in a sample depends upon its carbon content, i.e. the higher the total carbon, the higher the level of background [^{14}C]. To obtain a value for drug-related [^{14}C], the background level of [^{14}C] must be subtracted. All pre-dose samples were analyzed by AMS to obtain the background levels, which were used for background subtraction. Given the potential variability in the carbon content of homogenized feces and urine, all such samples underwent analysis using a FlashSmart Elemental Analyzer (Thermo Scientific, Waltham, Massachusetts, USA).

For AMS analysis, each sample, along with standards and controls, underwent combustion (oxidation) and graphitization (reduction). Radioactivity levels were then determined using a 250 KeV Single-Stage Accelerator Mass Spectrometer (NEC, Middleton, Wisconsin, USA).

Downloaded from dmd.aspetjournals.org at ASPET Journals on December 20, 2024

DMD Fast Forward. Published on October 29, 2024 as DOI: 10.1124/dmd.124.001895
This article has not been copyedited and formatted. The final version may differ from this version.

The mean Lower Limit of Quantification (LLOQ) was determined to be 0.12 pg tanimilast Equivalent/mL for urine measurements and 55 pg tanimilast Eq/g in feces samples.

Pharmacokinetics and statistical analysis

Due to the exploratory nature of the study, no formal sample size calculation was conducted. A sample size of 8 was selected to address the primary objectives of the study (Penner *et al.*, 2009). Analysis of plasma PK for non-radiolabeled tanimilast, [^{14}C]-tanimilast, and total-[^{14}C] in plasma was carried out at the Fortrea Clinical Research Unit (Leeds, UK). Non-compartmental analysis methods in Phoenix WinNonlin version 8.1.1 (Certara; New Jersey, USA) were employed for this purpose. PK variables were derived using the formulas provided in footnotes in Table 1. All descriptive statistical analyses were conducted using SAS version 9.4 (SAS Institute, Cary, North Carolina).

Bioanalysis of tanimilast. Blood samples were obtained from the non-dosing IV forearm and collected in vacuum tubes containing Lithium Heparin. Resolian (Cambridgeshire, UK) conducted the quantification of non-radiolabeled tanimilast in human plasma samples using a fully validated liquid chromatography tandem mass spectrometry (LC-MS/MS) method. Solid phase extraction, specifically Waters Oasis HLB 30 mg plates (Waters, Milford, Massachusetts, USA), was employed for sample purification. The internal standard (IS) for tanimilast comprised a stable-isotope-labeled [$^{2}H_6$]-tanimilast. The analytical instruments included a Xevo TQS mass spectrometer (Waters, Milford, Massachusetts, USA) and an ACQUITY UPLC system (Waters, Milford, Massachusetts, USA). Chromatographic separation utilized an ACQUITY BEH Phenyl column (1.7 µm, 100 x 2.1 mm; Waters) at 60°C, with a mobile phase composed of solvent A (0.1% formic acid in water) and solvent B (acetonitrile) at a flow rate of 0.85 mL/min. Retention time for tanimilast was 3.7 min, with a LLOQ set at 10 pg/mL.

Bioanalysis of total-[^{14}C]. The determination of total-[^{14}C] in plasma and whole blood employed the highly sensitive AMS method at Pharmaron ABS (Germantown, Maryland, USA). Prior to analysis, frozen samples were thawed at room temperature for approximately

Downloaded from dmd.aspetjournals.org at ASPET Journals on December 20, 2024

DMD Fast Forward. Published on October 29, 2024 as DOI: 10.1124/dmd.124.001895
This article has not been copyedited and formatted. The final version may differ from this version.

1 h, followed by vortex-mixing for 5 min at ~1500 rpm. Subsequently, samples were transferred to clean, small glass tubes containing pre-baked copper oxide powder. In cases where carbon content was insufficient, carbon carrier (Sodium benzoate, SB) was added to achieve a final carbon content of approximately 1.7 mg in the samples. All samples and controls underwent graphitization and were analyzed by AMS, with a mean LLOQ of 1.44 pg tanimilast Eq/mL.

Bioanalysis of [^{14}C]-tanimilast. The quantification of [^{14}C]-tanimilast in human plasma, urine, feces, and whole blood employed a validated LC+AMS assay. Each sample was fortified with a non-labeled internal standard (tanimilast) and subjected to solid phase extraction or liquid-liquid extraction, followed by LC fractionation and AMS analysis. The LLOQ for the LC+AMS assay was determined as 7.01 pg/mL for whole blood, 0.80 pg/mL for plasma, 9.88 pg/mL for feces, and 2.50 pg/mL for urine.

Metabolite profiling

The metabolite profiling in plasma was evaluated using time-proportional pools from each individual subject representing the area under the plasma concentration-time curve (AUC) from 0–72 hours ($AUC_{0–72h}$), approximately 60% of the $AUC_{0\text{-}240h}$ of total-[^{14}C]. Time-proportional pools were prepared for each matrix by combining volumes in accordance with the time intervals between individual samples, as previously described (Hamilton *et al.*, 1981; Hop *et al.*, 1998).

Homogenized feces and urine samples were pooled based on proportion to the amount (weight or volume) of excreta collected in each sampling period. The pool was made to represent at least 95% of the total-[^{14}C] excreted across all subjects, corresponding to samples collected between 0- and 144-hours post-dose for all subjects. A cross-subject pool was prepared by taking a constant proportion of each individual subject pool and combining to obtain a representative pooled feces and urine sample from all subjects. Only plasma and feces samples were extracted, with individual pools analyzed by AMS for total-[^{14}C] content. These concentrations, along with aliquot weights, were used to determine the total amount

Downloaded from dmd.aspetjournals.org at ASPET Journals on December 20, 2024

DMD Fast Forward. Published on October 29, 2024 as DOI: 10.1124/dmd.124.001895
This article has not been copyedited and formatted. The final version may differ from this version.

taken for extraction, after which the reconstituted extract was analyzed by AMS to calculate the recovered radioactivity (extraction efficiency). Plasma was extracted with methanol and both supernatant and re-solubilized plasma pellets were analyzed by AMS.

Chromatographic analysis was performed with an UHPLC Agilent 1290 (Agilent Technologies, Santa Clara, CA) using chromatographic method previously described (Cenacchi *et al.*, 2015). Radiochromatograms for plasma, feces, and urine were generated by collecting LC fractions, followed by AMS analysis of each fraction. AMS data (disintegrations per minute/fraction) and time-normalized data were imported into LAURA V6 (LabLogic Systems Ltd., Sheffield, UK) to generate radiochromatograms.

Regions of interest (ROI) were quantified and assigned to specific metabolites, wherever possible, from pools of plasma collected between 0 and 72 hours post-dose and from pools of urine or feces collected between 0 and 144 hours post-dose. Fractions measured below the LLOQ were treated as zero. In AUC plasma pools the %ROI is equivalent to the percentage of total-[^{14}C] exposure (area under the curve within 0-72 hours). In urine and feces, the %ROI was equivalent to percentage of total radioactivity and then calculated as the percentage of dose recovered in urine and feces between 0- and 144-hours post-dose.

Parent and metabolites assignments were established by matching retention times obtained via LC-UV with those eluting at the same retention time as the observed [^{14}C] peak. Metabolite identification was further supported by comparing adjusted relative retention times to existing data from previous preclinical and clinical studies (Cenacchi *et al.*, 2015).

Safety

Adverse events (AEs) were systematically recorded throughout the study, and safety was comprehensively evaluated. Full physical examinations were conducted at screening, Day -1 and before discharge. Hematology, blood chemistry, fasting glucose levels were assessed at screening, at pre-dose and before discharge, while vital signs and 12-lead electrocardiograms (ECG) were examined at screening, at pre-dose and 2.5 hours post-dose.

Downloaded from dmd.aspetjournals.org at ASPET Journals on December 20, 2024

DMD Fast Forward. Published on October 29, 2024 as DOI: 10.1124/dmd.124.001895
This article has not been copyedited and formatted. The final version may differ from this version.

Results

Demographic and Baseline Characteristics

16 subjects were screened, 8 were enrolled and all completed the study. The subjects' mean (standard deviation (SD)) age was 36.3 (4.4) years. Their mean (SD) body mass index was 28.1 (4.7) kg/m^2.

Mass Balance

Figure 1 displays the mean recovery of total-[^{14}C] over time following intravenous administration of [^{14}C]-tanimilast.

The overall average cumulative recovery in both feces and urine reached 78.9% (with individual values ranging from 75.2% to 82.7%) within the 240-hour period following the initiation of the infusion.

Feces accounted for 70.8% (individual range: 67.9% to 74.9%) of the total administered radioactivity while urine contributed for only 8.1% (individual range: 7.1% to 9.7%). Over 95% of radioactivity excreted in both feces and urine occurred within the initial 144 hours after the start of infusion. In the last collection period between 216 and 240-hours post-infusion initiation, feces and urine contained a mean of 0.03% and 0.18% of the administered radioactive dose, respectively.

On average, excretion of [^{14}C]-tanimilast in feces accounted for only 0.32% throughout a 240-hour period starting from the infusion commencement. [^{14}C]-tanimilast was measurable in feces for up to 96 hours post-dose in 5 out of 8 subjects, and it was quantifiable in 1 out of 8 subjects up to 144 hours after the initiation of infusion. Notably, [^{14}C]-tanimilast was not detectable in urine at any point in time.

Pharmacokinetics

After administering a nominal dose of 18.5 µg (500 nCi) [^{14}C]-tanimilast through IV, peak levels of both [^{14}C]-tanimilast and total-[^{14}C] in plasma exhibited similar patterns, with a median t_{max} of 0.22 hours (individual range: 0.17 to 0.25 hours) post-infusion initiation.

Downloaded from dmd.aspetjournals.org at ASPET Journals on December 20, 2024

DMD Fast Forward. Published on October 29, 2024 as DOI: 10.1124/dmd.124.001895
This article has not been copyedited and formatted. The final version may differ from this version.

Following attainment of maximum concentration (C_{max}), plasma concentrations of [^{14}C]-tanimilast and total-[^{14}C] demonstrated a multiphasic decline. The geometric mean terminal half-life ($t_{1/2}$) of [^{14}C]-tanimilast in plasma was approximately 14 hours (individual range: 6.4 to 33.1 hours), with quantifiable concentrations persisting up to 72 hours after infusion commencement in 3 out of 8 subjects (individual range: 0.849 to 1.120 pg/mL). The one subject that showed quantifiable [^{14}C]-tanimilast values in feces up to 144h, was the only one with quantifiable concentrations of [^{14}C]-tanimilast in plasma observed up to 96 hours post-infusion. Total-[^{14}C] in plasma showed a geometric mean $t_{1/2}$ of approximately 76 hours (individual range: 56.4 to 105.8 hours), and quantifiable concentrations were recorded at the last sampling time point, 240 hours after the start of infusion, in 7 out of 8 subjects (individual range: 2 to 18 pg Eq/mL). The geometric mean exposure of [^{14}C]-tanimilast, constituted approximately 13% of the total-[^{14}C] exposure in plasma as measured by area under curve extrapolated to infinity ($AUC_{0\text{-}inf}$).

The geometric mean clearance (CL) of [^{14}C]-tanimilast in plasma was determined to be 22.0 L/h, while in blood, it amounted to 43.2 L/h. The calculation of blood clearance was based on the blood-to-plasma ratio, computed at 20 minutes post-infusion initiation, yielding a geometric mean of 0.65 for total-[^{14}C] and 0.52 for [^{14}C]-tanimilast.

Since [^{14}C]-tanimilast was undetectable in urine, indicating negligible renal clearance, we inferred that hepatic clearance equated to blood clearance. The calculation of hepatic extraction ratio relied on blood clearance, considering a nominal hepatic blood flow value of 87 L/h (as per Davies and Morris, 1993), leading to a hepatic extraction (E_h) of 49.7%.

The geometric mean volume of distributions of [^{14}C]-tanimilast at the terminal phase (Vz) and at steady state (Vss), were 436.1 L and 212.6 L, respectively, while the mean residence time (MRT) was 9.15 h.

Finally, the geometric mean plasma CL of [^{14}C]-total was 2.94 L/h and corresponding blood CL was 4.91 L/h, the geometric mean Vz of [^{14}C]-total was 323.1 L.

Downloaded from dmd.aspetjournals.org at ASPET Journals on December 20, 2024

DMD Fast Forward. Published on October 29, 2024 as DOI: 10.1124/dmd.124.001895
This article has not been copyedited and formatted. The final version may differ from this version.

Regarding the administration of non-radiolabeled tanimilast, following a 3200 µg dose delivered through inhalation, the absorption kinetics was characterized by a rapid uptake, exhibiting a median t_{max} of 2.01 hours post-dose in plasma (individual range: 2.00 to 3.75 hours). Subsequent to reaching the C_{max}, plasma concentrations of tanimilast exhibited a biphasic decline, with a geometric mean $t_{1/2}$ longer than that observed with IV infusion of [^{14}C]-tanimilast, approximately 40 hours (individual range: 25.9 to 45.2 hours) (refer to Fig. 2, Table 1).

The estimated geometric mean absolute inhaled bioavailability of non-radiolabeled tanimilast, determined based on $AUC_{0\text{-}inf}$ when administered via inhalation in comparison to IV infusion, was 49.8% (individual range: 27.8% to 64.0%).

Notably, the between-subject variability for [^{14}C]-tanimilast, total-[^{14}C] and non-radiolabeled tanimilast in plasma was low, as assessed by the geometric coefficient of variation (CV%) for $AUC_{0\text{-}inf}$ and C_{max}, with values ranging from 18.6% to 28.4%.

Metabolite profiling

The radiochromatographic profiles and quantification of radioactive peaks in plasma, urine, and feces following [^{14}C]-tanimilast IV infusion are depicted in Figure 3.

The metabolic profiling in plasma was evaluated using time-proportional pooled samples collected from each individual subject between 0- and 72-hours post-dose. During this time frame, the radioactivity comprised over 60% of the total-[^{14}C] exposure as measured by $AUC_{0\text{-}240h}$, the recovery of radioactivity (extraction efficiency) from pooled plasma over the $AUC_{0\text{-}72h}$ period averaged 105%, with 50% recovered from the plasma supernatant and 55% from the protein pellet. Chromatographic retention times revealed [^{14}C]-tanimilast as the major radioactive compound in the pooled plasma extracts, constituting an average of 41.7% (individual range: 32.5% to 52.5%) of the 0-72 hours total-[^{14}C] exposure. Overall, no metabolites accounting for more than 5% of the 0-72 hours total-[^{14}C] were quantified. Ten metabolites were identified based on preclinical findings. These include CHF5956 (2.8%),

Downloaded from dmd.aspetjournals.org at ASPET Journals on December 20, 2024

DMD Fast Forward. Published on October 29, 2024 as DOI: 10.1124/dmd.124.001895
This article has not been copyedited and formatted. The final version may differ from this version.

formed by ester-hydrolysis; M5 (4.8%), formed by CHF5956 conjugation with glucuronic acid and loss of a chlorine atom; M9 (3.8%), formed by CHF5956 hydroxylation and loss of chlorine atom; M4 (4.4%), formed by CHF5956 hydroxylation, conjugation with glucuronic acid and loss of a chlorine atom; CHF5928 (4.3%), formed CHF5956 loss of N-oxide; M2 (1.8%), formed by CHF5956 conjugation with glucuronic acid and loss of the cyclopropylmethyl group; M3 (2.2%), formed by CHF5928 conjugation with glucuronic acid and loss of the cyclopropylmethyl group; M15 and/or M16 (1.5%), derived by tanimilast hydroxylation and conjugation with glucuronic acid (with loss of chlorine atom for M16); M38 (1.1%), formed by tanimilast hydroxylation and loss of the N-oxide; and M27 (2.1%), formed by tanimilast methylation (Table 2). Additionally, fourteen other radiochromatographic peaks, each accounting for less than 2% of the 0-72 hours total-[^{14}C], were identified but not structural characterized.

Metabolite profiling in urine and feces involved the analysis of pooled samples collected between 0- and 144-hours post-dose for all subjects. The radioactivity observed during this time frame constituted over 95% of the total-[^{14}C] recovered up to 240 hours post-dose and the extraction recovery of radioactivity from pooled homogenized feces (0-144h) was 82%. Twenty metabolites were quantified, and thirteen of them were identified based on preclinical findings. None of these metabolites exceeded 10% of the administered IV [^{14}C] dose.

Four metabolites were detected in both urine and feces: M3 (0.9% and 2.6% of administered dose respectively), M4 (1.7% and 2.0%, respectively), M5 (2.0% and 5.2%, respectively), and M9 (0.5% and 3.3%, respectively). Another metabolite identified in urine (M2, 1.6%) was also present in plasma. Unique metabolites identified in feces included M10 (2.5%), formed by tanimilast hydroxylation, conjugation with glutathione and loss of a chlorine atom, and M33 (4.4%), formed by tanimilast loss of N-oxide; and M25 (6.6%), formed by tanimilast hydroxylation, methylation and loss of a chlorine atom and of N-oxide, which could potentially co-elute with tanimilast. Other fecal metabolites included CHF5956, M15/M16, M38, CHF5928, and M27 (2.1%, 2.3%, 4.4%, 1.6%, and 1.6%, respectively). A putative metabolic pathway is proposed in Figure 4.

Downloaded from dmd.aspetjournals.org at ASPET Journals on December 20, 2024

DMD Fast Forward. Published on October 29, 2024 as DOI: 10.1124/dmd.124.001895
This article has not been copyedited and formatted. The final version may differ from this version.

Safety

No deaths, Severe Adverse Events, or noteworthy Adverse Events were documented throughout the course of the study. In general, only one participant reported experiencing three Treatment-emergent Adverse Events specifically, mild instances of abdominal pain lower, cough, and oropharyngeal pain. These events were mild in severity, resolved without treatment and were deemed unrelated to the treatment.

The analysis revealed no discernible patterns and no clinically significant observations in the clinical laboratory assessments, vital signs data, electrocardiogram (ECG) readings, or physical examination results throughout the duration of the study.

Downloaded from dmd.aspetjournals.org at ASPET Journals on December 20, 2024

DMD Fast Forward. Published on October 29, 2024 as DOI: 10.1124/dmd.124.001895
This article has not been copyedited and formatted. The final version may differ from this version.

Discussion

This study employed an innovative design to comprehensively analyze the ADME processes and essential PK parameters of inhaled tanimilast. Healthy male subjects received a single inhaled dose of non-radiolabeled drug and a concomitant [^{14}C]-labeled IV microtracer dose.

The study design enabled the examination of the inhaled availability of tanimilast, showing that, like other inhaled drugs (Daley-Yates *et al.*, 2001; Harrell *et al.*, 2019; Holmberg *et al.*, 2022), around 50% is absorbed into the systemic circulation. It is already demonstrated in animal model that oral bioavailability is negligible or extremely low (<1% in rat and monkey, and <7% in dogs (unpublished Chiesi data)), and tanimilast is a substrate of the human membrane transporters glycoprotein-P and BCRP, which may limit the gut permeability (Cenacchi *et al.*, 2018). Therefore, the quantity of tanimilast reaching the systemic circulation via the gastrointestinal route is reasonably significantly lower, or negligible, than the amount absorbed through the lungs. These findings substantiate absorption from the lungs as the primary route of bioavailable tanimilast absorption.

After IV administration, [^{14}C]-tanimilast reached its t_{max} at the conclusion of the infusion, with concentrations of the parent compound closely mirroring those of total-[^{14}C], at 631 pg/mL and 707 pg Eq/mL, respectively. This concurrence suggests that the radioactivity at peak concentration is exclusively attributed to [^{14}C]-tanimilast. Following attainment of the C_{max}, [^{14}C]-tanimilast displayed a $t_{1/2}$ significantly shorter than that of total-[^{14}C]. The overall exposure of [^{14}C]-tanimilast, constituting approximately 13% of the total-[^{14}C] exposure, serves as the initial indication of extensive metabolism occurring as elimination pathways. Notably, products of degradation persisted in the systemic circulation for an extended duration, albeit at very low concentrations, given that 240 hours post-IV administration, the total-[^{14}C] remained slightly above the LLOQ established by AMS. As indicated by 50% radioactivity recovery in the plasma supernatant from the 0-72h pool, drug-related materials may covalently bind to plasma proteins, which could explain the long half-life of total-[^{14}C], though the covalently bound fraction is inactive from a safety perspective.

Downloaded from dmd.aspetjournals.org at ASPET Journals on December 20, 2024

DMD Fast Forward. Published on October 29, 2024 as DOI: 10.1124/dmd.124.001895
This article has not been copyedited and formatted. The final version may differ from this version.

The PK of inhaled non-radiolabeled tanimilast compared to IV administration, revealed a significantly prolonged $t_{1/2}$ for the former (39 hours) compared to the latter (14 hours). This observation suggests that the absorption of tanimilast from the lung to the systemic circulation is the key determinant of its pharmacokinetic profile, with the lung acting as the primary reservoir. The short half-life of [^{14}C]-tanimilast in the systemic circulation, attributed to a high systemic clearance relative to the volume of distribution, underscores the rapid elimination of tanimilast once it enters the systemic circulation.

This data supports the tanimilast's design, maximizing lung retention, minimizing systemic exposure, and reducing class-related side effects common in PDE4 inhibitors. For instance, in COPD treatment, roflumilast, an oral PDE4 inhibitor, has limitations due to side effects such as gastrointestinal, psychiatric issues and weight loss (Rabe, 2011; Muñoz-Esquerre *et al.*, 2015; Rogliani *et al.*, 2016). Roflumilast is rapidly metabolized into its active metabolite, roflumilast N-oxide, which accounts for about 90% of its PDE4 inhibitory activity (Lahu *et al.*, 2008). Roflumilast N-oxide exhibits higher systemic exposure compared to tanimilast (Bethke *et al.*, 2007), along with much lower protein binding (Lahu *et al.*, 2008; Armani *et al.*, 2014; Han *et al.*, 2023). Consequently, the systemic exposure of the free fraction - responsible for systemic effects - is much higher for roflumilast at therapeutic doses.

The analysis of [^{14}C]-tanimilast in whole blood, plasma, urine, and feces has provided valuable insights into the elimination routes of tanimilast. The systemic clearance, defined as the sum of renal and hepatic components, was evaluated. Remarkably, [^{14}C]-tanimilast was undetectable in urine, rendering renal clearance negligible. This observation supports the assumption that the elimination of the drug predominantly occurs through the hepatic route. By establishing that total systemic clearance equals hepatic clearance, the blood-to-plasma ratio of [^{14}C]-tanimilast was determined, allowing for the derivation of systemic clearance in blood. Subsequently, hepatic extraction was estimated to be approximately 50%. Notably, the recovery of [^{14}C]-tanimilast in feces was minimal (0.3% of total), suggesting that the majority of tanimilast is eliminated by the liver through metabolism rather than excretion. Hence, also consistent with other findings including observations from animal models

Downloaded from dmd.aspetjournals.org at ASPET Journals on December 20, 2024

DMD Fast Forward. Published on October 29, 2024 as DOI: 10.1124/dmd.124.001895
This article has not been copyedited and formatted. The final version may differ from this version.

(Cenacchi *et al.*, 2015), liver metabolism is emerging as the predominant route for the elimination of tanimilast.

The mean retrieval of intravenously administered radioactivity averaged 79%, with 71% of it retrieved in feces and 8% in urine. Over 95% of the radioactivity was excreted within the initial 144 hours. A comprehensive analysis of metabolites was conducted using LC+AMS on pooled fractions containing the predominant radioactivity in plasma (0-72 h), urine and feces (0-144 h). Plasma samples revealed that the primary component was unchanged [^{14}C]-tanimilast, constituting 42% of the pooled radioactivity. Further analysis identified 24 potential metabolites, each below 5% of the drug-related exposure, highlighting their minimal contribution to overall circulating radioactivity. The examination of plasma-derived metabolites implicated crucial biotransformation pathways, specifically phase I reactions involving ester-group hydrolysis and hydroxylation, potentially mediated by carboxylesterases and cytochrome P-450, respectively. This was followed by phase II conjugation reactions with glucuronic acid. CHF5956, the product of tanimilast hydrolysis, exhibited a potency in human peripheral blood mononuclear cells (PBMCs) at least 2000-fold lower than tanimilast, also CHF5928 exhibited a potency less than 6-fold lower than CHF5956 (Armani et al., 2014 and unpublished Chiesi data), suggesting that the other identified metabolites are unlikely to be associated with any significant pharmacological activity. As study limitation, it was not possible to measure the ester-hydrolysis product counterpart and its related metabolic pathway due to the position of the radiocarbon in the molecule. Another limitation is the identification of metabolites based on preclinical findings, due to the minimal [^{14}C]-material quantification for thorough metabolite characterization in this study. All biotransformations were observed in preclinical models, with some, such as oxidative dechlorination, also found in humans using roflumilast having a similar chemical structure
(http://www.accessdata.fda.gov/drugsatfda_docs/nda/2011/022522Orig1s000MedR.pdf).
Additional research would be necessary to validate the chemical structure of metabolites present at very low concentrations.

Downloaded from dmd.aspetjournals.org at ASPET Journals on December 20, 2024

DMD Fast Forward. Published on October 29, 2024 as DOI: 10.1124/dmd.124.001895
This article has not been copyedited and formatted. The final version may differ from this version.

Notably, the M3(R2) guidance from the International Committee on Harmonization (https://database.ich.org/sites/default/files/M3_R2__Guideline.pdf) specifies that if a metabolite exceed 10% of the circulating drug-related exposure or administered dose in excreta, additional non-clinical evaluation of the metabolite should be considered. Given the linear, time-independent pharmacokinetics (Jolling *et al.*, 2019) of tanimilast shown in earlier studies, a single-dose design was deemed appropriate for metabolite profiling in this study. Furthermore, when considering drugs with a daily administered dose of less than 10 mg, larger fractions of the drug-related material may be more appropriate signals for testing. Considering tanimilast having a maximum therapeutic total daily dose of 3.2 mg (1.6 mg twice a day), our analysis revealed that none of the tanimilast metabolites exceeded the critical 10% threshold in plasma, urine or feces.

This innovative study design employing administration of IV [^{14}C]-labeled microtracer concomitantly with an inhaled pharmacological dose, contributes to optimizing drug development and holds ethical implications. The benefits include 1) reducing the radioactivity administered to humans, addressing potential safety concern; 2) minimizing the number of studies required for a comprehensive characterization of the ADME profile, PK, and metabolite profiling; 3) and eliminating the need for intravenous toxicology programs and dosimetry studies in animals, aligning with the principles of the 3Rs (Replacement, Reduction, Refinement) developed as a framework for ethical and human animal research (Hubrecht and Carter, 2019; Young *et al.*, 2023).

A limitation of current study design might be the incomplete quantitative recovery of administered radioactivity, with an average retrieval of intravenously administered radioactivity slightly below 80%. Tanimilast showed a long total-[^{14}C] elimination half-life (>50 h) and the main excretion route is through feces, these properties could explain the slightly lower recovery than the target threshold 80% for human mass balance studies (Roffey *et al.*, 2007). At the final collection point, the recovered dose in both feces and urine was less than 1%, suggesting that extending the collection period would unlikely improve recovery rates. Considering the labelling position in the chemical structure, it seems unlikely the formation of

Downloaded from dmd.aspetjournals.org at ASPET Journals on December 20, 2024

DMD Fast Forward. Published on October 29, 2024 as DOI: 10.1124/dmd.124.001895
This article has not been copyedited and formatted. The final version may differ from this version.

^{14}C-CO_2 and a subsequent loss of radioactivity through expiration. In a rat study (unpublished Chiesi data), after 120 hours, less than 1% of the radioactivity remained in the carcass, suggesting no irreversible tissue binding. Metabolite profiling was conducted on pools containing most of the radioactivity. While quantification rates of metabolites may be subject to subtle changes when considered relative to the total-[^{14}C], this is not expected to have a significant impact, as metabolites were well below the critical 10% threshold set by regulatory guidelines.

In conclusion, our study demonstrates that inhaled tanimilast absorption from the lungs serves as the primary route of bioavailable tanimilast absorption, with rate-limited pulmonary absorption. Tanimilast is swiftly eliminated by the liver through metabolism upon reaching the systemic circulation, supporting the intended design to maximize exposure and retention within the lung. Notably, [^{14}C]-tanimilast remained the major circulating compound, with negligible recovery in feces and no detectable metabolites necessitating further qualification. The study's integrated design enables a comprehensive characterization of tanimilast's ADME and PK in a single trial, supporting an optimized path for clinical development and regulatory application in respiratory conditions.

Downloaded from dmd.aspetjournals.org at ASPET Journals on December 20, 2024

DMD Fast Forward. Published on October 29, 2024 as DOI: 10.1124/dmd.124.001895
This article has not been copyedited and formatted. The final version may differ from this version.

Conflicts of interest

Michele Bassi, Veronica Puviani, Debora Santoro, Sonia Biondaro, Aida Emirova, Mirco Govoni are employees of Chiesi, the sponsor of this study.

Authorship Contributions

Participated in research design: Bassi, Puviani, Santoro, Biondaro, Emirova, Govoni

Conducted experiments: Bassi

Performed data analysis: Bassi, Santoro, Govoni

Wrote or contributed to the writing of the manuscript: Bassi, Puviani, Santoro, Biondaro, Emirova, Govoni

Acknowledgments

The authors thank Dr. Giandomenico Brogin from Chiesi Farmaceutici for contributing with the preclinical data.

Data availability statement

Chiesi commits to sharing with qualified scientific and medical Researchers, conducting legitimate research, patient-level data, study-level data, the clinical protocol and the full clinical study report of Chiesi Farmaceutici S.p.A.-sponsored interventional clinical trials in patients for medicines and indications approved by the European Medicines Agency and/or the US Food and Drug Administration after 1st January 2015, following the approval of any received research proposal and the signature of a Data Sharing Agreement. Chiesi provides access to clinical trial information consistently with the principle of safeguarding commercially confidential information and patient privacy. Other information on Chiesi's data sharing commitment, access and research request's approval process are available in the Clinical Trial Transparency section of http://www.chiesi.com/en/research-and-development/.

Downloaded from dmd.aspetjournals.org at ASPET Journals on December 20, 2024

DMD Fast Forward. Published on October 29, 2024 as DOI: 10.1124/dmd.124.001895
This article has not been copyedited and formatted. The final version may differ from this version.

References

Ambery C, Young G, Fuller T, Lazaar AL, Pereira A, Hughes A, Ramsay D, van den Berg F, and Daley-Yates P (2018) Pharmacokinetics, Excretion, and Mass Balance of [14 C]-Batefenterol Following a Single Microtracer Intravenous Dose (Concomitant to an Inhaled Dose) or Oral Dose of Batefenterol in Healthy Men. *Clin Pharmacol Drug Dev* **7**:901–910.

Armani E, Amari G, Rizzi A, Fanti R De, Ghidini E, Capaldi C, Carzaniga L, Caruso P, Guala M, Peretto I, La Porta E, Bolzoni PT, Facchinetti F, Carnini C, Moretto N, Patacchini R, Bassani F, Cenacchi V, Volta R, Amadei F, Capacchi S, Delcanale M, Puccini P, Catinella S, Civelli M, and Villetti G (2014) Novel Class of Benzoic Acid Ester Derivatives as Potent PDE4 Inhibitors for Inhaled Administration in the Treatment of Respiratory Diseases. *J Med Chem* **57**:793–816.

Bethke TD, Böhmer GM, Hermann R, Hauns B, Fux R, Mörike K, David M, Knoerzer D, Wurst W, and Gleiter CH (2007) Dose-Proportional Intraindividual Single- and Repeated-Dose Pharmacokinetics of Roflumilast, an Oral, Once-Daily Phosphodiesterase 4 Inhibitor. *The Journal of Clinical Pharmacology* **47**:26–36.

Cenacchi V, Battaglia R, Cinato F, Riccardi B, Spinabelli D, Brogin G, Puccini P, and Pezzetta D (2015) In vitro and in vivo metabolism of CHF6001, a selective phosphodiesterase (PDE4) inhibitor. *Xenobiotica* **45**:693–710.

Cenacchi V, Salvadori M, Riccardi B, Brogin G, Ghiglieri A, Messina M, Imre G, and Puccini P (2018) Role of efflux transporters in the absorption, distribution and elimination in rodents of a novel PDE4 inhibitor, CHF6001. *European Journal of Pharmaceutical Sciences* **115**:100–108.

Coppola P, Andersson A, and Cole S (2019) The Importance of the Human Mass Balance Study in Regulatory Submissions. *CPT Pharmacometrics Syst Pharmacol* **8**:792–804.

Downloaded from dmd.aspetjournals.org at ASPET Journals on December 20, 2024

DMD Fast Forward. Published on October 29, 2024 as DOI: 10.1124/dmd.124.001895
This article has not been copyedited and formatted. The final version may differ from this version.

Daley-Yates PT, Price AC, Sisson JR, Pereira A, and Dallow N (2001) Beclomethasone dipropionate: absolute bioavailability, pharmacokinetics and metabolism following intravenous, oral, intranasal and inhaled administration in man. *Br J Clin Pharmacol* **51**:400–409.

Davies B, and Morris T (1993) Physiological parameters in laboratory animals and humans. *Pharm Res* **10**:1093–1095.

Facchinetti F, Civelli M, Singh D, Papi A, Emirova A, and Govoni M (2021) Tanimilast, A Novel Inhaled PDE4 Inhibitor for the Treatment of Asthma and Chronic Obstructive Pulmonary Disease. *Front Pharmacol* **12**.

Fontana E, Cenacchi V, Pivetti F, Pignatti A, Pazzi T, Bondanza L, and Pazzi M (2017) Synthesis of ^{14}C- and ^{2}H-labelled CHF6001: A new potent PDE4 inhibitor. *J Labelled Comp Radiopharm* **60**:577–585.

Govoni M, Bassi M, Santoro D, Donegan S, and Singh D (2023) Serum IL-8 as a Determinant of Response to Phosphodiesterase-4 Inhibition in Chronic Obstructive Pulmonary Disease. *Am J Respir Crit Care Med* **208**:559–569.

Govoni M, Bassi M, Vezzoli S, Lucci G, Emirova A, Nandeuil MA, Petruzzelli S, Jellema GL, Afolabi EK, Colgan B, Leaker B, Kornmann O, Beeh KM, Watz H, and Singh D (2020) Sputum and blood transcriptomics characterisation of the inhaled PDE4 inhibitor CHF6001 on top of triple therapy in patients with chronic bronchitis. *Respir Res* **21**:72.

Hamilton RA, Garnett WR, and Kline BJ (1981) Determination of mean valproic acid serum level by assay of a single pooled sample. *Clin Pharmacol Ther* **29**:408–413.

Han M, Lin X, Cui G, Chen S, Wu W, Mi N, Wang J, Xiao C, Zhang X, Lu X, and Li J (2023) A Single-center, Open-label, Parallel Control Study Comparing the Pharmacokinetics and Safety of a Single Oral Dose of Roflumilast and Its Active Metabolite Roflumilast N-oxide in Healthy Chinese and Caucasian Volunteers. *Clin Pharmacol Drug Dev* **12**:314–323.

Downloaded from dmd.aspetjournals.org at ASPET Journals on December 20, 2024

DMD Fast Forward. Published on October 29, 2024 as DOI: 10.1124/dmd.124.001895
This article has not been copyedited and formatted. The final version may differ from this version.

Harrell AW, Wilson R, Man YL, Riddell K, Jarvis E, Young G, Chambers R, Crossman L, Georgiou A, Pereira A, Kenworthy D, Beaumont C, Marotti M, Wilkes D, Hessel EM, and Fahy WA (2019) An Innovative Approach to Characterize Clinical ADME and Pharmacokinetics of the Inhaled Drug Nemiralisib Using an Intravenous Microtracer Combined with an Inhaled Dose and an Oral Radiolabel Dose in Healthy Male Subjects. *Drug Metabolism and Disposition* **47**:1457–1468.

Holmberg AA, Weidolf L, Necander S, Bold P, Sidhu S, Pelay-Gimeno M, de Ligt RAF, Verheij ER, Jauhiainen A, Psallidas I, Wählby Hamrén U, and Prothon S (2022) Characterization of Clinical Absorption, Distribution, Metabolism, and Excretion and Pharmacokinetics of Velsecorat Using an Intravenous Microtracer Combined with an Inhaled Dose in Healthy Subjects. *Drug Metabolism and Disposition* **50**:150–157.

Hop CECA, Wang Z, Chen Q, and Kwei G (1998) Plasma-Pooling Methods To Increase Throughput for in Vivo Pharmacokinetic Screening. *J Pharm Sci* **87**:901–903.

Hubrecht, and Carter (2019) The 3Rs and Humane Experimental Technique: Implementing Change. *Animals* **9**:754.

International Commission on Radiological Protection (1991) Principles for Intervention for Protection of the Public in a Radiological Emergency. A report of a Task Group of Committee 4 of the International Commission on Radiological Protection. *Ann ICRP* **22**:1–30.

Jolling K, Äbelö A, Luyckx N, Nandeuil M, Govoni M, Cella M, and Lindauer A (2019) Concentration–QT Modeling Following Inhalation of the Novel Inhaled Phosphodiesterase-4 Inhibitor CHF6001 in Healthy Volunteers Shows an Absence of QT Prolongation. *CPT Pharmacometrics Syst Pharmacol* **8**:460–468.

Lahu G, Huennemeyer A, von Richter O, Hermann R, Herzog R, McCracken N, and Zech K (2008) Effect of Single and Repeated Doses of Ketoconazole on the Pharmacokinetics of Roflumilast and Roflumilast N-Oxide. *The Journal of Clinical Pharmacology* **48**:1339–1349.

Downloaded from dmd.aspetjournals.org at ASPET Journals on December 20, 2024

DMD Fast Forward. Published on October 29, 2024 as DOI: 10.1124/dmd.124.001895
This article has not been copyedited and formatted. The final version may differ from this version.

Lappin G (2016) Approaches to intravenous clinical pharmacokinetics: Recent developments with isotopic microtracers. *The Journal of Clinical Pharmacology* **56**:11–23.

Mariotti F, Govoni M, Lucci G, Santoro D, and Nandeuil MA (2018) Safety, tolerability, and pharmacokinetics of single and repeat ascending doses of CHF6001, a novel inhaled phosphodiesterase-4 inhibitor: two randomized trials in healthy volunteers. *Int J Chron Obstruct Pulmon Dis* **Volume 13**:3399–3410.

Muñoz-Esquerre M, Diez-Ferrer M, Montón C, Pomares X, López-Sánchez M, Huertas D, Manresa F, Dorca J, and Santos S (2015) Roflumilast added to triple therapy in patients with severe COPD: A real life study. *Pulm Pharmacol Ther* **30**:16–21.

Penner N, Klunk LJ, and Prakash C (2009) Human radiolabeled mass balance studies: objectives, utilities and limitations. *Biopharm Drug Dispos* **30**:185–203.

Rabe KF (2011) Update on roflumilast, a phosphodiesterase 4 inhibitor for the treatment of chronic obstructive pulmonary disease. *Br J Pharmacol* **163**:53–67.

Roffey SJ, Obach RS, Gedge JI, and Smith DA (2007) What is the Objective of the Mass Balance Study? A Retrospective Analysis of Data in Animal and Human Excretion Studies Employing Radiolabeled Drugs. *Drug Metab Rev* **39**:17–43.

Rogliani P, Calzetta L, Cazzola M, and Matera MG (2016) Drug safety evaluation of roflumilast for the treatment of COPD: a meta-analysis. *Expert Opin Drug Saf* **15**:1133–1146.

Singh D, Bassi M, Balzano D, Lucci G, Emirova A, Anna Nandeuil M, Jellema G, Afolabi EK, Leaker B, Kornmann O, Michael Beeh K, Watz H, and Govoni M (2021) COPD patients with chronic bronchitis and higher sputum eosinophil counts show increased type-2 and PDE4 gene expression in sputum. *J Cell Mol Med* **25**:905–918.

Singh D, Beeh KM, Colgan B, Kornmann O, Leaker B, Watz H, Lucci G, Geraci S, Emirova A, Govoni M, and Nandeuil MA (2019) Effect of the inhaled PDE4 inhibitor CHF6001 on biomarkers of inflammation in COPD. *Respir Res* **20**:180.

Downloaded from dmd.aspetjournals.org at ASPET Journals on December 20, 2024

DMD Fast Forward. Published on October 29, 2024 as DOI: 10.1124/dmd.124.001895
This article has not been copyedited and formatted. The final version may differ from this version.

Singh D, Emirova A, Francisco C, Santoro D, Govoni M, and Nandeuil MA (2020) Efficacy and safety of CHF6001, a novel inhaled PDE4 inhibitor in COPD: the PIONEER study. *Respir Res* **21**:246.

Singh D, Leaker B, Boyce M, Nandeuil MA, Collarini S, Mariotti F, Santoro D, and Barnes PJ (2016) A novel inhaled phosphodiesterase 4 inhibitor (CHF6001) reduces the allergen challenge response in asthmatic patients. *Pulm Pharmacol Ther* **40**:1–6.

Singh D, Watz H, Beeh KM, Kornmann O, Leaker B, Colgan B, Lucci G, Emirova A, Nandeuil MA, Santoro D, Balzano D, and Govoni M (2020) COPD sputum eosinophils: relationship to blood eosinophils and the effect of inhaled PDE4 inhibition. *European Respiratory Journal* **56**:2000237.

Spracklin DK, Chen D, Bergman AJ, Callegari E, and Obach RS (2020) Mini-Review: Comprehensive Drug Disposition Knowledge Generated in the Modern Human Radiolabeled ADME Study. *CPT Pharmacometrics Syst Pharmacol* **9**:428–434.

Young GC, and Croft M (2020) AMS in drug development: Exploring the current utility of AMS and future opportunities for absolute bioavailability and ADME investigations, in *Identification and Quantification of Drugs, Metabolites, Drug Metabolizing Enzymes, and Transporters* pp 185–210, Elsevier.

Young GC, Spracklin DK, James AD, Hvenegaard MG, Pedersen ML, Wagner DS, Georgi K, Schieferstein H, Bjornsdottir I, Romeo AA, Cassidy KC, Da-violante G, Blech S, Schulz SI, Cuyckens F, Nguyen MA, and Scarfe G (2024) Non-Labeled, Stable Labeled, or Radiolabelled Approaches for Provision of Intravenous Pharmacokinetics in Humans: A Discussion Piece. *Clin Pharmacol Ther* **115**:931–938.

Young GC, Spracklin DK, James AD, Hvenegaard MG, Scarfe G, Wagner DS, Georgi K, Schieferstein H, Bjornsdottir I, van Groen B, Romeo AA, Cassidy KC, Da-violante G, Bister B, Blech S, Lyer R, Schulz SI, Cuyckens F, and Moliner P (2023) Considerations for Human ADME Strategy and Design Paradigm Shift(s) – An Industry White Paper. *Clin Pharmacol Ther* **113**:775–781.

Downloaded from dmd.aspetjournals.org at ASPET Journals on December 20, 2024

DMD Fast Forward. Published on October 29, 2024 as DOI: 10.1124/dmd.124.001895
This article has not been copyedited and formatted. The final version may differ from this version.

Footnotes

Funding: This study was funded by Chiesi.

Reprint requests: Michele Bassi, Global Clinical Development, Chiesi Farmaceutici SpA, Largo Francesco Belloli 11/A - 43122 Parma (Italy). Email: m.bassi@chiesi.com

Citation: partial results of this study were presented at the 2023 ERS International Congress: Bassi M, Puviani V, Santoro D, Biondaro S, Emirova A, and Govoni M (2023) Characterization of the ADME profile of tanimilast following administration of an intravenous microtracer combined with a single inhaled dose in healthy males, European Respiratory Journal; 62: Suppl. 67, PA1293.

Downloaded from dmd.aspetjournals.org at ASPET Journals on December 20, 2024

DMD Fast Forward. Published on October 29, 2024 as DOI: 10.1124/dmd.124.001895
This article has not been copyedited and formatted. The final version may differ from this version.

Figure legends

Figure 1: *Arithmetic mean (+SD) cumulative recovery of total radioactivity in excreta over time following intravenous infusion of 18.5 µg (500 nCi) [^{14}C]-tanimilast*

Figure 2: *Geometric mean plasma concentrations profiles following inhalation of 3200 µg tanimilast and intravenous infusion of [^{14}C]-tanimilast 18.5 µg (500 nCi)*

Figure 3: *Radiochromatograms generated from multiple injection of A) plasma pool extracts (AUC0-72h); B) cross subject pooled urines (0-144 h); C) cross subject pooled feces extract (0-144 h). DPM, disintegrations/min.*

Figure 4: *Putative metabolic scheme for tanimilast in human following IV administration. The asterisk indicates the position of the ^{14}C label in Tanimilast.*

Downloaded from dmd.aspetjournals.org at ASPET Journals on December 20, 2024

DMD Fast Forward. Published on October 29, 2024 as DOI: 10.1124/dmd.124.001895
This article has not been copyedited and formatted. The final version may differ from this version.

Tables

Table 1: *Summary of PK parameters following 3200 µg inhaled tanimilast and 18.5µg of intravenous [^{14}C]-tanimilast*

PK Parameter	Tanimilast (inhaled, N=8)	[^{14}C]-Tanimilast (IV, N=8)	Total-[^{14}C] (IV, N=8)
C_{max} (pg/mL)	1979 (22.5)	631 (19.1)	707 (21.6) ‡
AUC_{0-t} (pg·h/mL)	71088 (28.2)	783 (18.2)	5403 (16.7) ‡
AUC_{0-inf} (pg·h/mL)	72403 (28.4)	814 (18.6)	6083 (19.6) ‡+
T_{max} (h) median (range)	2.00 (2.00–3.75)	0.217 (0.17–0.25)	0.217 (0.17–0.25)
$t_{1/2}$ (h)	39.30 (18.2)	13.74 (55.1)	76.09 (23.1)+
CL (L/h)	21.99 (18.6)*	22.00 (18.6)	2.94 (19.6)*
Vz (L)	1247.5 (27.0)*	436.1 (38.6)	323.1 (27.0)*+
Vss (L)	--	201.3 (36.2)	--
Blood:Plasma Ratio	--	0.517 (54.9)+	0.649 (23.9)+
E_h*	--	0.497 (53.5)+	--
MRT AUC (h)*	--	9.15 (49.3)	--
F AUC, %	49.8 (26.8)	--	--

All values are geometric mean (CV%) unless otherwise specified.

Cmax, the value of maximum plasma concentration; AUC, area under the curve; AUC0-t, the area under the concentration-time curve from dosing to the last quantifiable concentration; tmax, time from dosing of the maximum plasma concentration; t1/2, terminal phase half-life; CL, total body plasma clearance; Vz, volume of distribution; Vss, volume of distribution at steady state; Eh, hepatic extraction ratio; MRT, mean residence time of the unchanged drug in the systemic circulation; F, absolute inhaled bioavailability; PK, pharmacokinetics; CV%, percentage of coefficient of variation.

*The values were calculated post hoc.

Downloaded from dmd.aspetjournals.org at ASPET Journals on December 20, 2024

DMD Fast Forward. Published on October 29, 2024 as DOI: 10.1124/dmd.124.001895
This article has not been copyedited and formatted. The final version may differ from this version.

$MRT = AUMC_{0\text{-}inf} / AUC_{0\text{-}inf}$

$E_h = (CL_{total} - CL_{renal})/Q_H$

$Vss = Dose_{iv} \times AUMC_{0\text{-}inf} / (AUC_{0\text{-}inf})^2$

$F = [(AUC_{0\text{-}inf})_{inhaled} \times Dose_{iv}] / [(AUC_{0\text{-}inf})_{iv} \times Dose_{inhaled}]$

+n=6

‡Units expressed as pg tanimilast Eq/mL

Downloaded from dmd.aspetjournals.org at ASPET Journals on December 20, 2024

DMD Fast Forward. Published on October 29, 2024 as DOI: 10.1124/dmd.124.001895
This article has not been copyedited and formatted. The final version may differ from this version.

Table 2: *Quantification and putative identification of the major radioactive metabolites in urine, feces (0-144h) and plasma following intravenous administration of [^{14}C]-tanimilast*

Name	Proposed modification	% of dose in urine	% of dose in feces	% of drug-related exposure in plasma (0-72h)
M2	CHF5956 conjugation with glucuronic acid and loss of the cyclopropylmethyl group	1.6		1.8
M3	CHF5928 conjugation with glucuronic acid and loss of the cyclopropylmethyl group	0.9	2.6	2.2
M4	CHF5956 hydroxylation, conjugation with glucuronic acid and loss of a chlorine atom	1.7	2.0	4.4
M5	CHF5956 conjugation with glucuronic acid and loss of a chlorine atom	2.0	5.2	4.8
M9	CHF5956 hydroxylation and loss of chlorine atom	0.5	3.3	3.8
M10	Tanimilast hydroxylation, conjugation with glutathione and loss of a chlorine atom		2.5	
CHF5956	Tanimilast ester-hydrolysis		2.1	2.8
M15 and/or	Tanimilast hydroxylation		2.3	1.5

Downloaded from dmd.aspetjournals.org at ASPET Journals on December 20, 2024

DMD Fast Forward. Published on October 29, 2024 as DOI: 10.1124/dmd.124.001895
This article has not been copyedited and formatted. The final version may differ from this version.

M16	and conjugation with glucuronic acid (M15) with loss of chlorine atom (M16)		
M38	Tanimilast hydroxylation and loss of the N-oxide	4.4	1.1
CHF5928	CHF5956 loss of N-oxide	1.6	4.3
M25[a]	Tanimilast hydroxylation, methylation and loss of a chlorine atom and N-oxide	6.6	
Tanimilast			41.7
M27	Tanimilast methylation	1.6	2.1
M33	Tanimilast loss of the N-oxide	4.4	

a: potentially co-eluted with tanimilast

Downloaded from dmd.aspetjournals.org at ASPET Journals on December 20, 2024

Figure 1

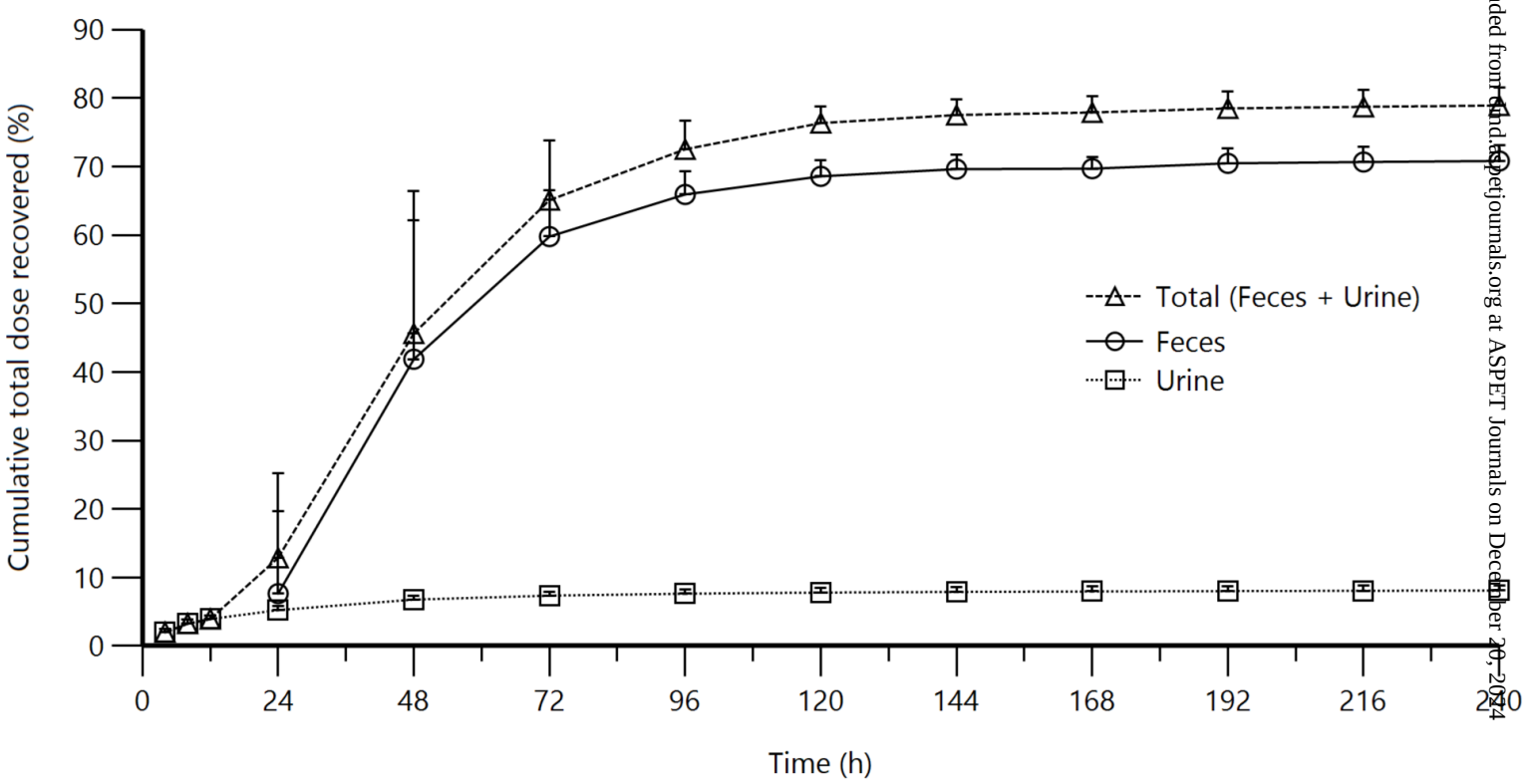

Downloaded from dmd.aspetjournals.org at ASPET Journals on December 20, 2024

Figure 2

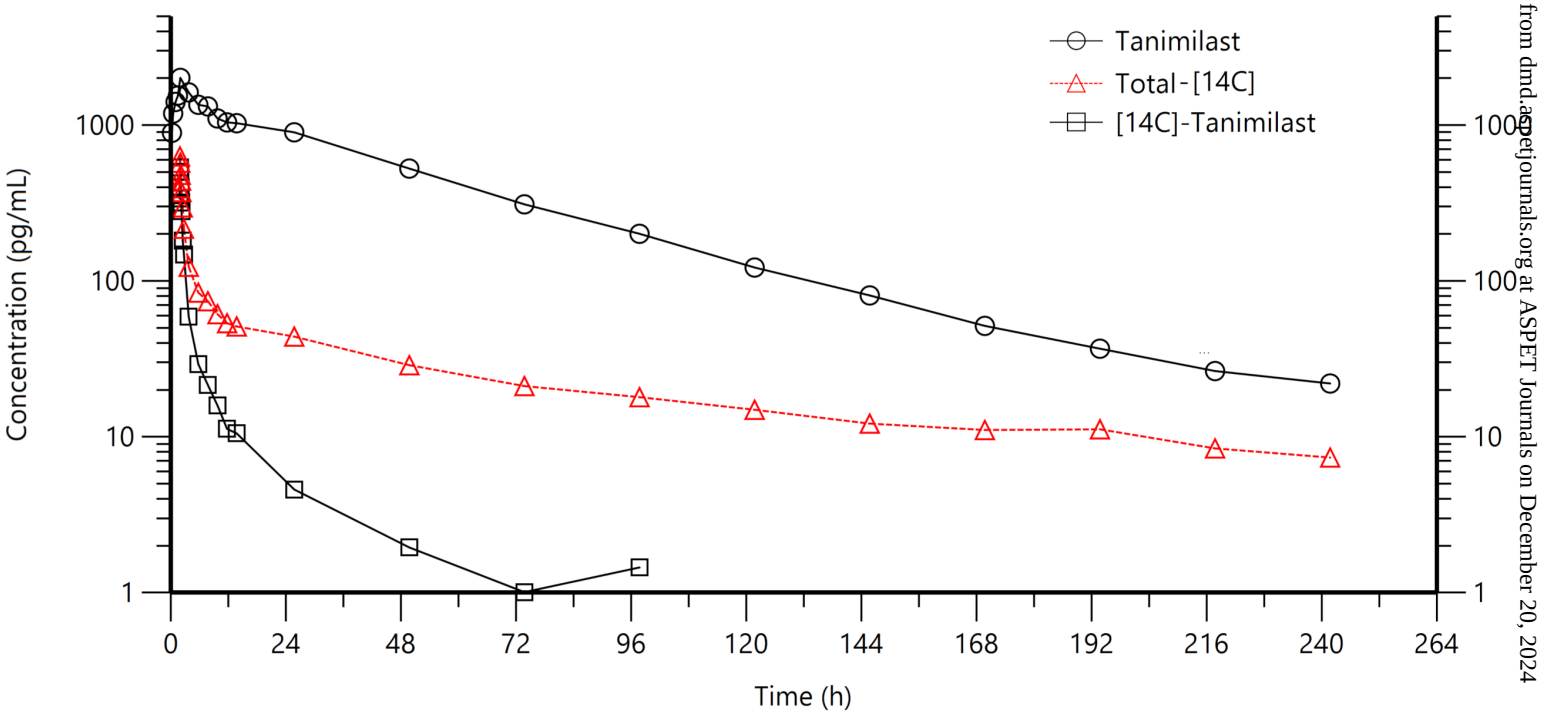

Downloaded from dmd.aspetjournals.org at ASPET Journals on December 20, 2024

Figure 3

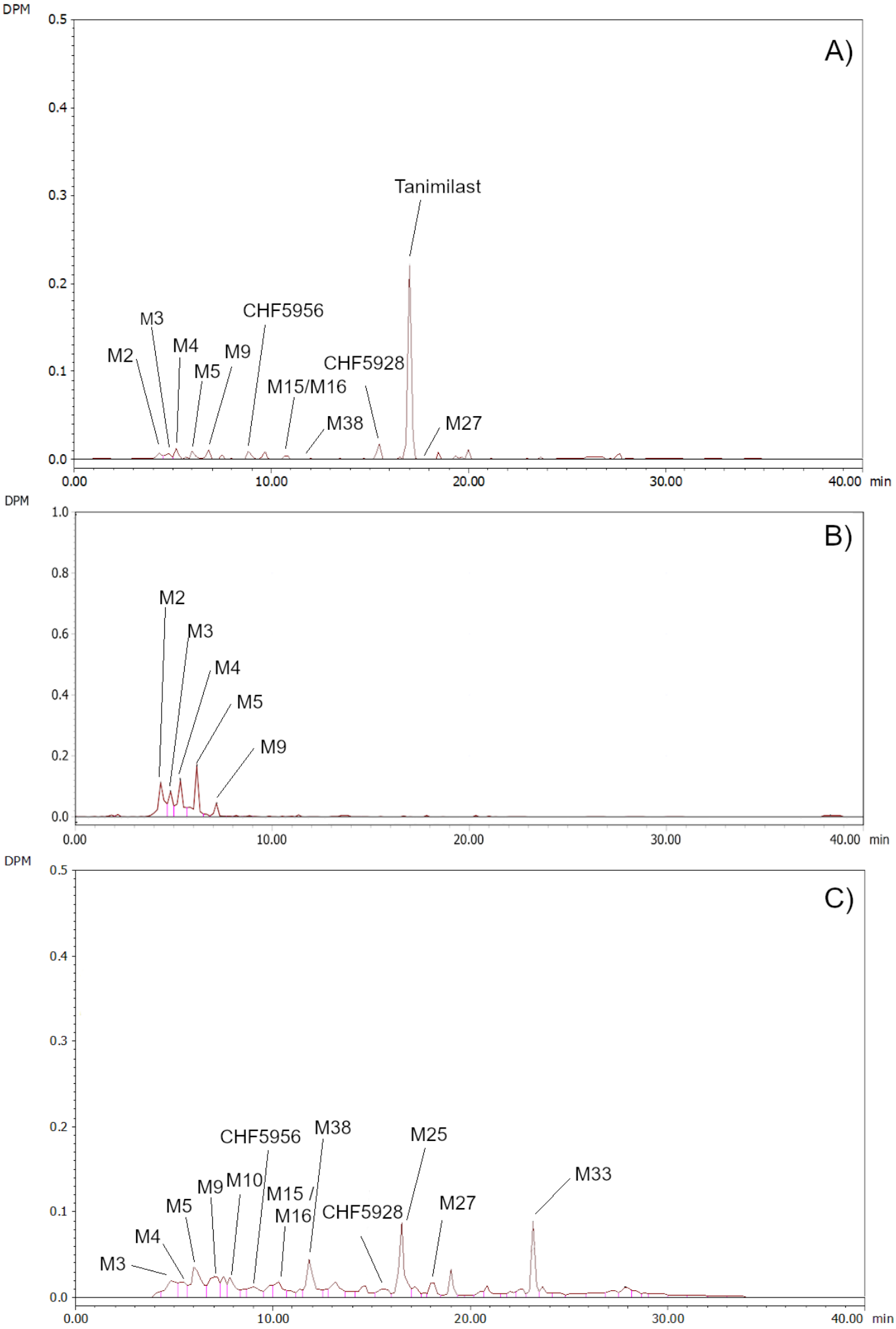

Downloaded from dmd.aspetjournals.org at ASPET Journals on December 20, 2024

Figure 4

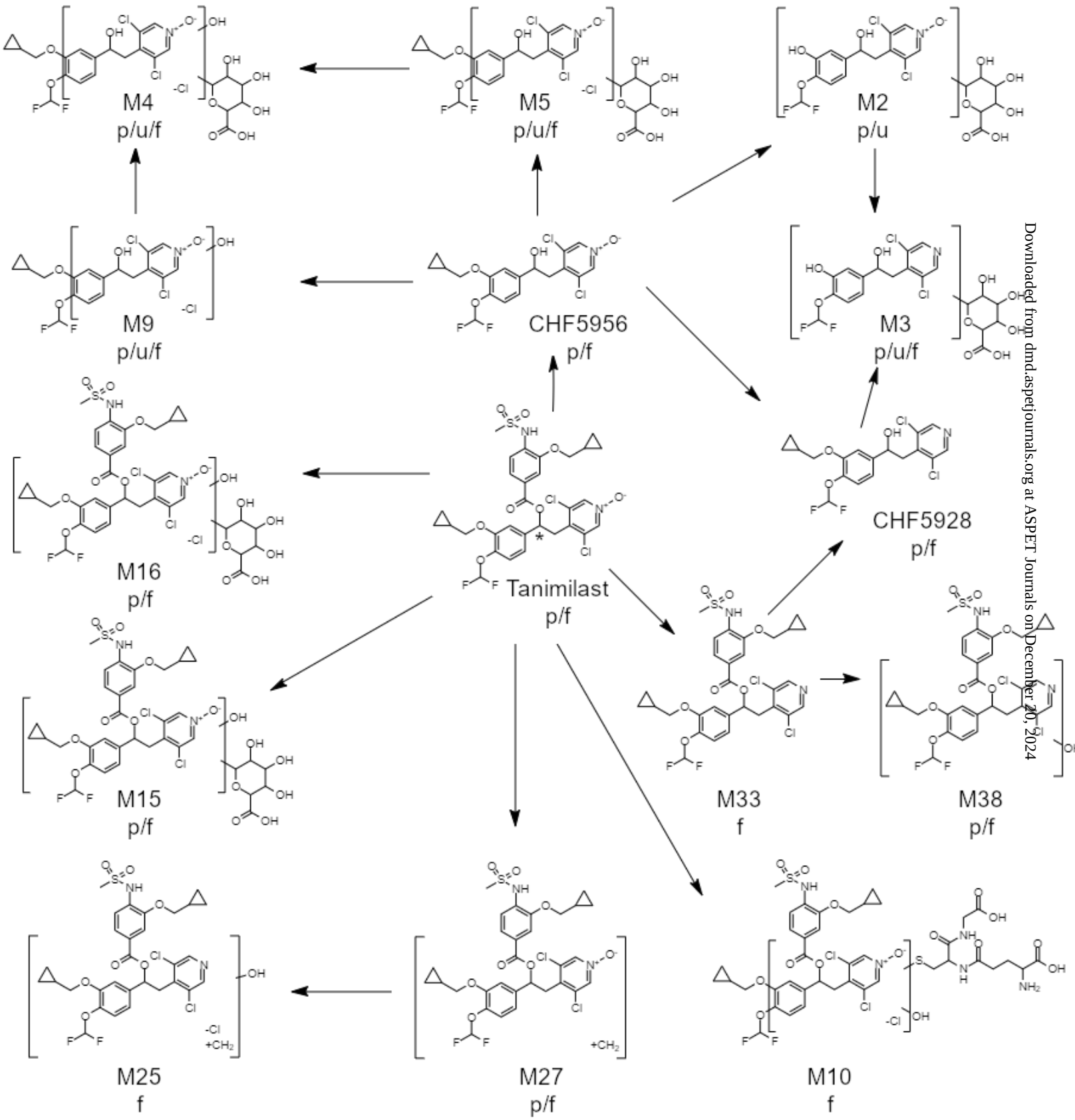

Downloaded from dmd.aspetjournals.org at ASPET Journals on December 20, 2024